

MOL # 37093

## **Nicotine glucuronidation and the human UDP-glucuronosyltransferase UGT2B10\***

Sanna Kaivosari, Päivi Toivonen, Leah M. Hesse, Mikko Koskinen, Michael H. Court, and  
Moshe Finel

*Department of Pharmacokinetics and Bioanalytics, Orion Corporation Orion Pharma, P.O. Box 65, 02101 Espoo, Finland (S.K., P.T., M.K.); Division of Pharmaceutical Chemistry, Faculty of Pharmacy, University of Helsinki, P.O. Box 56, 00014 University of Helsinki, Finland (S.K., P.T.); Molecular Pharmacogenetics Laboratory, Department of Pharmacology and Experimental Therapeutics, Tufts University School of Medicine, Boston, USA (L.M.H., M.H.C.); Drug Discovery and Development Technology Center (DDTC), Faculty of Pharmacy, University of Helsinki, P.O. Box 56, 00014 University of Helsinki, Finland (M.F.)*

### \*Footnote

This research was supported by the Academy of Finland (projects 207535 and 210933) and the Sigrid Juselius Foundation. Dr Court is supported by grants GM-61834 and GM-74369 from the National Institute of General Medical Sciences, National Institutes of Health, Bethesda, Maryland, USA. Dr Hesse is the recipient of an F32 Ruth Kirschstein postdoctoral fellowship training award (AA-15647) from the National Institute on Alcohol Abuse and Alcoholism, National Institutes of Health, Bethesda, Maryland, USA.

MOL # 37093

## Running title page

Running title: nicotine glucuronidation and the human UGT2B10

Corresponding author: Moshe Finel, DDTC, Faculty of Pharmacy, University of Helsinki,

P.O.Box 56 (Viikinkaari 5), 00014 University of Helsinki, Finland

Tel. +358 (0)9 19159193, Fax +358 (0)9 19159556, E-mail: moshe.finel@helsinki.fi

Number of text pages:

Number of tables: 0

Number of figures: 8

Number of references: 28

Number of words in Abstract: 230

Number of words in Introduction: 627

Number of words in Discussion: 1048

## Abbreviations

HIM, human intestine microsomes; HLM, human liver microsomes; LC-MS, liquid chromatography - mass spectrometry; UDPGA, UDP-glucuronic acid; UGT, UDP-glucuronosyltransferase.

MOL # 37093

## Abstract

Nicotine biotransformation affects the smoking habits of addicted individuals and therefore their health risk. Using an improved analytical method, we have discovered that the human UDP-glucuronosyltransferase (UGT) 2B10, a liver enzyme previously unknown to conjugate nicotine or exhibit considerable activity towards any compound, plays a major role in nicotine inactivation by direct conjugation with glucuronic acid at the aromatic nitrogen atom. The  $K_m$  of recombinant UGT2B10 for nicotine (0.29 mM) was similar to that determined for human liver microsomes (0.33 mM), whereas the  $K_m$  of UGT1A4 for nicotine was almost 10-fold higher (2.4 mM). UGT2B10 was also more active than UGT1A4 in N-glucuronidation of cotinine (oxidative nicotine metabolite), while UGT2B7 exhibited only low nicotine glucuronidation activity and was essentially inactive towards cotinine. UGT1A9 did not glucuronidate nicotine or cotinine. Quantitative RT-PCR showed that UGT2B10 mRNA was exclusively expressed in human liver, while UGTs 1A4 and 2B7 were expressed at comparable, although somewhat lower, levels in liver and several other extrahepatic tissues including kidney and intestine. These findings for UGT2B10 (but not for UGT1A4 and UGT2B7) were mirrored by human tissue activities since nicotine and cotinine glucuronidation rates in intestine microsomes were less than 0.1% that of human liver microsomes. These novel findings solve two seemingly separate questions, namely which is the UGT that is primarily responsible for nicotine glucuronidation in human liver, and what conjugation reactions are catalyzed by UGT2B10.

MOL # 37093

## Introduction

Nicotine is not carcinogenic by itself and might even have some beneficial therapeutic effects in some neurological diseases. Nonetheless, it is the major perpetrator of tobacco-related diseases since nicotine addiction drives smokers to pursue the habit despite the known health hazards. Nicotine concentration in the blood rises sharply during cigarette smoking, and then declines rapidly due to metabolism and clearance, driving the addicted individual to reach for another cigarette. Hence, better understanding of nicotine metabolism can assist the development of treatments to reduce the health risks associated with nicotine addiction.

Cytochrome P450 monooxygenase 2A6 (CYP2A6) catalyzes nicotine oxygenation and plays an important role in nicotine metabolism (Hukkanen et al., 2005; Nakajima and Yokoi, 2005). However, there is more to nicotine metabolism than CYP2A6 since both nicotine and its primary oxidation metabolite, cotinine, undergo direct *N*-glucuronidation at the aromatic nitrogen (Fig. 1) (Ghosheh et al., 2001; Ghosheh and Hawes, 2002a). Glucuronidation is catalyzed by one or more of the human liver UDP-glucuronosyltransferases (UGTs) (Radomska-Pandya et al., 1999; Tukey and Strassburg, 2000; Wells et al., 2004). The UGTs are membrane-bound enzymes of the endoplasmic reticulum that catalyze glucuronic acid transfer from UDP-glucuronic acid (UDPGA) to a large variety of aglycones, both endogenous compounds and xenobiotics. There are some 19 human UGTs that are divided into two families, UGT1 (or UGT1A) and UGT2, based on sequence homology and gene structure (Mackenzie et al., 2005). The expression of UGTs is tissue specific. However, most UGTs are expressed in more than one tissue and nearly each human tissue that contains UGTs, carry more than a single UGT isoform (Tukey and Strassburg, 2000; Mackenzie et al., 2003). Nonetheless, the liver is the major site of glucuronidation in our body and most UGTs, but not all, are expressed in liver cells.

MOL # 37093

The substrate specificity of the human UGTs is highly complex. Most human UGTs can glucuronidate several different compounds with variable chemical structure, albeit at different kinetics (Uchaipichat et al., 2004). This leads to partial overlap in the substrate specificity of individual UGTs. However, alongside individual human UGTs that are well documented to metabolize many different aglycones with high activity, there are also a few UGTs which so far have demonstrated either no activity (or only very limited activity) when screened against a large variety of aglycone substrates. These so-called “orphan”, or nearly orphan, UGTs include UGT2B10, UGT2B11 (Turgeon et al., 2003), UGT1A5 (Finel et al., 2005), and perhaps also UGT2B28 (Lévesque et al., 2001).

The UGTs mostly catalyze the conjugation of an hydroxyl group in the aglycone substrate with glucuronic acid from the co-substrate UDPGA. However, some UGTs can also conjugate other functional groups such as different amines (Green and Tephly, 1998; Hawes, 1998; Zenser et al., 2002; Borlak et al., 2006). Nicotine is one of several xenobiotics that are subjected to direct N-glucuronidation when incubated with human liver microsomes in the presence of UDPGA (Ghosheh et al., 2001). A primary question concerning nicotine glucuronidation is which enzyme catalyzes this reaction. Several laboratories have tried to identify the main nicotine glucuronidating human UGT, but this undertaking turned out to be highly challenging (Ghosheh and Hawes, 2002a; Nakajima et al., 2002; Kuehl and Murphy, 2003). Among the tested human UGTs, UGT1A4, an enzyme “specializing” in *N*-glucuronidation, was the most efficient in cotinine glucuronidation (Kuehl and Murphy, 2003; Nakajima and Yokoi, 2005). However, it was also concluded that the contribution of UGT1A4 to nicotine glucuronidation may be minor and another, not yet identified UGT, may play a significant role in nicotine metabolism (Ghosheh and Hawes, 2002a; Kuehl and

MOL # 37093

Murphy, 2003; Nakajima and Yokoi, 2005). Armed with an improved analytical method, and prompted by several incidental observations about the little-studied UGT2B10 (Girard et al., 2005), we set out to solve this enduring question regarding nicotine metabolism.

MOL # 37093

## Materials and Methods

**Materials.** (-)-Nicotine hydrogen tartrate salt, (-)-cotinine, alamethicin (from *Trichoderma viride*), and D-saccharic acid 1,4-lactone were purchased from Sigma-Aldrich. UDPGA (as triammonium salt) was from Fluka Chemie (Buchs, Switzerland). Nicotine-N- $\beta$ -glucuronide hydrate, nicotine-N- $\beta$ -glucuronide(-methyl-d3), cotinine-N- $\beta$ -D-glucuronide, and (R,S)-cotinine-N- $\beta$ -D-glucuronide(-methyl-d3) were purchased from Toronto Research Chemicals, Toronto, Canada. Pooled human liver microsomes (HLM, 18 donors) and pooled human intestine microsomes (HIM) were from BD Biosciences (Bedford, MA). According to the manufacturer, the intestine microsomes were prepared from both the duodenum and jejunum sections of 5 different donors and so they could be regarded as small intestine microsomes. As a positive control for the UGTs in the two different human microsomes samples, they were subject to activity assays in the presence of 100  $\mu$ M. The entacapone glucuronidation activity in HIM was high (27% of substrate was converted to entacapone glucuronide using 0.3 mg/ml microsomal protein activated with alamethicin, and 1 hour incubation time), and it was 29% of the glucuronidation activity measured in HLM under the same incubation conditions.

**Recombinant human UGTs** were produced in baculovirus-infected insect cells as previously described (Kurkela et al., 2003; Kurkela et al., 2007). The relative expression levels of UGT1A4, UGT1A9, UGT2B7, and UGT2B10 in the test samples were determined simultaneously by immunodetection using a tetra-His monoclonal antibody (Qiagen, Hilden, Germany) as detailed elsewhere (Kurkela et al., 2007).

**UGT mRNA expression in human tissues.** Total RNA was extracted using Trizol reagent (Sigma-Aldrich, St Louis, MO, USA) from 47 human livers and pooled. Liver donors were all of European-American ancestry and included both males (n=36) and females (n=11). Use of

MOL # 37093

the tissue was approved by the institutional review board of Tufts University School of Medicine. Total RNA from human kidney (male African-American donor), small intestine (5 European-American donors), colon (3 European-American donors), trachea (male European-American donor), lung (male African-American donor), and whole brain (male African-American donor) were purchased from BD-Clontech (USA), while total RNA from human stomach (male European-American donor) was from Ambion (USA). To generate cDNA, 1  $\mu$ g of total RNA was treated with DNase enzyme (Promega, USA) and then reverse transcribed (Superscript II, Invitrogen, USA) with random hexamer primer (0.1  $\mu$ g) according to the manufacturers' protocol. Quantitative PCR reactions (25  $\mu$ L) included Sybr Green 2X master mix (Applied Biosystems, USA), 10  $\mu$ L of 1:10 diluted cDNA (except 1:30 dilution for liver cDNA; and 1:500 to 1:1500 dilution for cDNA assayed with 18S rRNA primers), and 200 nM of each primer. Primer pair sequences were as follows: CCC CTC GAT GCT CTT AGC TGA GTG T (18S-rRNA-forward), CGC CGG TCC AAG AAT TTC ACC TCT (18S-rRNA-reverse), TGC GCC ACA AAG GAG CCA AAC AT (UGT2B10-forward), ATG ATA AAT AGC ACG GTT GCC ACA CAA (UGT2B10-reverse), GTT ACG CTG GGC TAC ACT CAA GG (UGT1A4-forward), CTC CAC ACA ACA CCT ATG AAG GG (UGT1A4-reverse), TTT CAC AAG TAC AGG AAA TCA TGT CAA T (UGT2B7-forward), CAG CAG CTC ACT ACA GGG AAA AAT (UGT2B7-reverse). Real-time PCR analysis (Model 7300, Applied Biosystems, USA) was performed with the following PCR method: 95°C for 10 min, 40-45 cycles of 95°C for 30 sec and 60°C for 60 sec. Amplification specificity was ensured initially by sequencing of representative PCR products, and in each run by PCR product duplex melting temperature analysis. Negative controls included exclusion of cDNA template and reverse transcription enzyme. mRNA concentrations were calculated using standard curves of PCR threshold cycle number versus concentration of template, which were derived from serial dilutions of purified PCR product. Curves were found to be linear ( $R^2 >$



MOL # 37093

0.99) over the concentration range  $10^{-9}$  to  $10^{-14}$  M for 18S rRNA and  $10^{-14}$  to  $10^{-18}$  M for other gene products, which defined the upper and lower quantitation limits of the respective assays. For each tissue, cDNA reactions were performed in triplicate and quantitative PCR reactions were performed at least in duplicate. Results were expressed as the mean (SE) number of mRNA copies per  $10^9$  copies of 18S rRNA. Assay precision as reflected by the coefficient of variation of replicates averaged 19%, 18%, and 23% for UGT1A4, UGT2B7, and UGT2B10, respectively.

**Activity assays.** The incubation mixtures contained 100 mM phosphate buffer pH 7.4, 5 mM  $MgCl_2$ , 0.2-1 mg protein/ml recombinant UGTs, HLM or HIM, 5 mM UDPGA, and 0.1, 0.5 or 4 mM nicotine or cotinine. Alamethicin (100  $\mu$ g/mg of microsomal protein) was added to HLM and HIM incubations, but not to incubations with recombinant UGTs. The kinetic assays were performed typically at 10 concentrations of nicotine or cotinine, 0.005-4 mM. Under the assay conditions, metabolite formation was shown to be linear with respect to both protein concentration (0.2 mg protein/ml for HLM, 1 mg protein/ml for HIM and recombinant UGTs) and incubation time (60-120 min). The reactions were initiated by the addition of UDPGA, incubated at 37°C for 60-120 min and terminated by protein precipitation with trifluoroacetic acid while the incubates were kept in an ice-water bath. Following centrifugation, internal standard (methyl-d3-nicotine glucuronide or (R,S)-methyl-d3-cotinine glucuronide) was added, and the samples were subjected to LC-MS analysis. The apparent kinetic parameters  $K_m$  and  $V_{max}$  were estimated by nonlinear regression analysis using SigmaPlot Enzyme Kinetics Module v. 1.1 (SPSS Inc., Chicago, IL). The conventional Michaelis-Menten equation was fitted to initial velocity data without weighting factors. The goodness of the fit was evaluated by visual inspection of the Eadie-Hofstee plots, the standard errors of the parameters, and  $R^2$  values.

MOL # 37093

**LC-MS analyses.** The samples were analyzed using an Agilent series 1100 liquid chromatograph (Agilent, Waldbronn, Germany) with a thermostated column compartment at 30°C using a Discovery HS F5 100x2.1 mm C18 column (Sigma-Aldrich) and a 20x4.0 mm guard column of the same material. The mobile phase consisted of two solvents, methanol and trifluoroacetic acid in water, pH 2.2, and the flow rate was 0.2 ml/min. The proportion of methanol increased linearly from 5% to 30% during the 15 min gradient run. The glucuronides were monitored by Agilent 1100 series single quadrupole mass spectrometer (model G-1946A) with atmospheric pressure electrospray ionization using the following settings: N<sub>2</sub> as drying gas (13.0 L/min, 350°C), nebulizer pressure 50 psig, V<sub>cap</sub>(pos) 4 kV, and fragmenter voltage 150 V. Nicotine glucuronide and the internal standard methyl-d<sub>3</sub>-nicotine glucuronide were monitored as [M+H]<sup>+</sup> ions at *m/z* 339 and 342, respectively, and both eluted at approximately 6.3 min retention time (Fig. 2). Cotinine glucuronide and the internal standard (R,S)-methyl-d<sub>3</sub>-cotinine glucuronide were monitored as [M+H]<sup>+</sup> ions at *m/z* 353 and 356, respectively. The retention time of cotinine glucuronide was approximately 8.3 min, while (R,S)-methyl-d<sub>3</sub>-cotinine glucuronide eluted in two peaks between 8.5 and 9 min. Since the two peaks of the diastereomeric internal standard were inseparable in the LC stage of the analysis, the peak area sum of them was used in the internal standardization. Nicotine and cotinine glucuronides were quantified by comparing peak area ratios (analyte/internal standard) to the peak area ratios generated with a standard curve.

MOL # 37093

## Results

We have developed an improved LC-MS method to quantify with high sensitivity and specificity the nicotine and cotinine N-glucuronidation activity of recombinant UGTs. In previous studies there were clear difficulties in measuring this activity (Ghosheh and Hawes, 2002a; Nakajima et al., 2002), mainly due to a combination of low rates of nicotine glucuronidation by recombinant UGTs, and insensitive analytical methods. Using a pentafluorophenylpropyl bonded column and a trifluoroacetic acid – methanol gradient, we obtained good column retention even for the highly hydrophilic nicotine and cotinine glucuronides (Fig. 2), compounds that otherwise have very poor retention by conventional C<sub>18</sub> columns. In addition to chromatographic improvements, we took advantage of the relatively high sensitivity of MS detection and incorporated commercially available glucuronide standards and deuterated internal standards to enhance accuracy. Using this newly developed method, we were able to quantify as little as 5 nM (corresponding to UGT activity of 0.04 pmol/min/mg) of nicotine glucuronide formed in the samples and 10 nM (0.08 pmol/min/mg) of cotinine glucuronide.

Our newly developed analytical method was applied to the determination of nicotine and cotinine glucuronidation rates by UGT1A4 and UGT1A9, enzymes previously reported to catalyze nicotine glucuronidation (Kuehl and Murphy, 2003), as well as by UGT2B7, an enzyme that is involved in the glucuronidation of many structurally diverse xenobiotics including N-glucuronidation reactions (Zhang et al., 2004; Xu et al., 2006). Importantly, the activity of UGT2B10 was also determined since our preliminary studies with this enzyme showed efficient *N*-glucuronidation of certain other compounds (manuscript in preparation). In the course of these experiments it was noticed that the activity of recombinant UGT2B10 sharply declines upon the isolation of microsomal membranes from insect cells (Fig. 3). We

MOL # 37093

have, thus, skipped the step of microsomal membrane isolation and thereafter switched to the use of cell homogenates in activity determinations for the recombinant UGT2B10. In addition, the assays of UGT1A9 and UGT2B7 that are reported here were performed using cell homogenates. In the case of UGT1A4, however, the measurements were performed using microsomal membranes since the normalized activity in both preparations was very similar (Fig. 3) and previous studies on nicotine glucuronidation employed equivalent preparations (Kuehl and Murphy, 2003).

The relative expression level of each of these recombinant UGTs was measured by immunodetection (see Methods) in order to allow better comparison of their glucuronidation activity by adjusting them to the relative amount of enzyme in each sample (i.e. normalization of expression level). The relative expression levels per mg protein in the sample (either cell homogenate or microsomal membranes), ranged from 1.0 for UGT1A4, through 1.8 and 2.1 for UGT2B10 and UGT2B7, respectively, and up to 4.5 for UGT1A9.

The results of the nicotine and cotinine glucuronidation analyses are presented in Fig. 2. Three different substrate concentrations, 0.1, 0.5 and 4 mM, were used in these activity assays and the major result of these experiments was that the human UGT2B10 is the most active human UGT in both nicotine and cotinine glucuronidation, at least as far as normalized activity is concerned (Figs. 4A and 4B). In line with the previous report (Kuehl and Murphy, 2003), UGT1A4 exhibited detectable N-glucuronidation of both nicotine and cotinine, but only at the two higher substrate concentrations (Fig. 4A). The analyses of UGT1A9 did not reveal any nicotine or cotinine glucuronidation activity, but we have detected low level of nicotine glucuronidation by UGT2B7 (Fig. 4A). The cotinine glucuronidation activity of UGT1A4 was similar to its activity towards nicotine, whereas cotinine glucuronidation by

MOL # 37093

UGT2B10 at lower substrate concentrations was significantly below its rate of nicotine glucuronidation (Fig. 2B), suggesting lower affinity of this enzyme for cotinine (see below). Cotinine glucuronidation by UGT2B7 was below the quantification limit.

Kinetic analyses were performed for nicotine and cotinine glucuronidation by recombinant UGTs 1A4 and 2B10, as well as by human liver microsomes (HLM). Large differences were observed between recombinant UGTs and HLM in glucuronidation rates of both nicotine and cotinine (Fig. 5). This difference is possibly due to a lower concentration of fully active enzyme in SF9 cell membranes, resulting from a limited capacity of insect cells to support correct folding and/or post-translation modification of heterologously expressed UGTs. The  $K_m$  values, however, are independent of the enzyme concentration and provide a useful tool to compare recombinant UGTs with the native enzymes in HLM. These kinetic analyses revealed a marked difference in the affinities of UGT1A4 and HLM for nicotine, while the  $K_m$  of UGT2B10 for nicotine was very similar to the corresponding value of HLM (Fig. 5A). In the case of cotinine glucuronidation, the  $K_m$  values of UGT1A4, UGT2B10 and HLM were quite similar to each other (Fig. 5B). Despite this, the expression-normalized cotinine glucuronidation activity of recombinant UGT2B10 was significantly higher than that of UGT1A4 (Fig. 4B).

Expression levels of UGT2B10, UGT1A4 and UGT2B7 in selected tissues were determined using a highly sensitive and quantitative RT-PCR method (Fig. 6). The results were particularly interesting with respect to UGT2B10 since, at least at the level of mRNA, this gene was exclusively expressed in human liver and at levels similar to UGT1A4 and UGT2B7. UGTs 1A4 and 2B7, on the other hand, were also expressed at significant levels in several of the other tested tissues, including kidney, small intestine, colon and trachea (Fig.

MOL # 37093

6). Of particular note is that both UGT1A4 and UGT2B7 were expressed in the small intestine at about 10% of the level of that in liver, while UGT2B10 was not detected (i.e. less than 1 copy of UGT2B10 mRNA per  $10^9$  copies of 18S rRNA; or less than 0.05% of the liver level). This latter finding provided us with a unique, although indirect, method to demonstrate that the native UGT2B10 (not merely the recombinant enzyme), is the main human UGT responsible for nicotine glucuronidation through comparison of nicotine glucuronidation activities in human liver and intestine microsomes, as follows.

Nicotine and cotinine glucuronidation rates were determined in pooled samples of human microsomes from either the liver (HLM, 18 donors) or the small intestine (HIM, 5 donors). The results revealed very low but quantifiable nicotine glucuronidation activity in HIM (Fig. 5B), something that was not previously reported (Ghosheh and Hawes, 2002b), probably due to the lower sensitivity of the methods used earlier. Nevertheless, the nicotine glucuronidation activity in the small intestine was only about 0.1% that of the nicotine activity in the liver (Fig. 7A, note the different scale on the Y axes), a result which mirrored the tissue differences in UGT2B10 mRNA levels, but not UGT1A4 or 2B7 mRNA levels (see above). Cotinine glucuronidation by HIM was below the limit of quantification, while in HLM it was at the same range as the nicotine glucuronidation rate (Figs. 7A and 7B). In agreement with the kinetic analyses (Fig. 5), the dependence of cotinine glucuronidation rate by HLM on substrate concentration was different than the nicotine glucuronidation rate of these microsomes (Fig. 7A).

Taken together, these results strongly suggest that UGT2B10 is the major UGT isoform mediating nicotine N-glucuronidation in human liver.

MOL # 37093

## Discussion

Nicotine is the major culprit in tobacco-related diseases, causing smokers to pursue their habit despite the known health hazards. Understanding nicotine biotransformation in our body is therefore both interesting and important. Finding which of the human UGTs is primarily responsible for N-glucuronidation of nicotine has been a highly challenging objective in the past (Ghosheh and Hawes, 2002a; Nakajima et al., 2002; Kuehl and Murphy, 2003), much more than is regularly encountered when glucuronidation is studied. Clarifying this issue is, therefore, expected to contribute significantly to our understanding of the substrate specificity of UGTs, particularly with respect to such N-glucuronidation reactions.

The improved analytical method to study nicotine glucuronidation contributed significantly to the new finding. Nonetheless, a major clue came from preliminary studies that showed recombinant human UGT2B10 can catalyze more efficient N-glucuronidation of some substrates that are only poorly glucuronidated by recombinant UGT1A4 (Kaivosari, Koskinen and Finel, unpublished observation). We have also noticed that the activity of recombinant UGT2B10 is sensitive to the regular procedure for the isolation of microsomes from the baculovirus-infected insect cells, a finding that may partly explain why the glucuronidation activity of this enzyme was barely detected in past works (Turgeon et al., 2003; Girard et al., 2005). Consequently, until now, UGT2B10 was largely assumed to be an “orphan” enzyme. The finding reported here may prompt other investigators to rethink and re-examine the involvement of UGT2B10 in the metabolism and clearance of a number of xenobiotics, particularly those undergoing N-glucuronidation.

It may be premature to speculate at this point as to the reasons leading to the higher activity of UGT2B10 in whole cell homogenates versus microsomal membrane preparations (Fig. 3).

MOL # 37093

Experiments with different recombinant UGTs production systems must be carried out before one can conclude with confidence whether or not this is only a characteristic of UGT2B10 expressed in baculovirus-infected insect cells. Nevertheless, we suggest that regardless the source of recombinant UGTs, future studies on the glucuronidation of different compounds will include cell homogenates, alongside isolated microsomes, at least at the screening stages.

UGT2B10 is not the only human enzyme capable of nicotine glucuronidation and until this work it was assumed that UGT1A4 is responsible for most of this activity in human liver microsomes (Kuehl and Murphy, 2003; Nakajima and Yokoi, 2005). In addition, UGT1A9 was reported to exhibit such activity (Kuehl and Murphy, 2003). While our results question the role of UGT1A9 in N-glucuronidation of nicotine, they clearly confirm the activity of UGT1A4 and also demonstrate low but detectable nicotine glucuronidation activity by UGT2B7 (Fig. 4A). Nonetheless, the present findings strongly suggest that UGT2B10, rather than either UGT1A4 or UGT2B7, plays the major role in nicotine glucuronidation.

Evidence that UGT2B10 is responsible for hepatic N-glucuronidation of nicotine as well as a major contributor to cotinine glucuronidation is derived from two major lines of experimentation. In the case of recombinant UGTs, the activity assays clearly demonstrate that the normalized activity of UGT2B10 is much higher than that of UGT1A4 or UGT2B7 for both nicotine and cotinine glucuronidation (Fig. 4). Moreover, the  $K_m$  value of UGT2B10 for nicotine was similar to the corresponding  $K_m$  in HLM, whereas in UGT1A4 this value was much higher (Fig. 5). In addition, the qRT-PCR results although not a direct measure for the content of the different UGTs in HLM, suggest that the amount of UGT2B10 in the liver is considerable and in the same range as UGT1A4 and UGT2B7, if not higher (Fig. 6).



MOL # 37093

In the case of native enzymes expressed in human tissues, our results support previous finding that the major site of nicotine glucuronidation in the human body is the liver (Ghosheh and Hawes, 2002b). In combination with the qRT-PCR results (Fig. 6), the very low nicotine glucuronidation found in HIM (Fig. 7), suggest that neither UGT1A4 nor UGT2B7 play a major role in hepatic nicotine glucuronidation. On the other hand, the correlation between the tissue nicotine glucuronidation activity (Fig. 7) to the expression level of UGT2B10 (Fig. 6) is striking. This is very strong circumstantial evidence that native UGT2B10 is indeed responsible for hepatic nicotine glucuronidation, in full agreement with the results from recombinant UGTs (Figs. 4 and 5).

Knowing now that UGT2B10 is specifically active in the N-glucuronidation of certain compounds raises the question as to what makes UGT2B10 and UGT1A4 rather specialized in this type of conjugation reaction. This contrasts with several other enzymes, such as UGT1A3 and UGT2B7 that can catalyze the N-glucuronidation of certain aglycones in addition to other glucuronidation reactions (Green and Tephly, 1998; Zenser et al., 2002; Zhang et al., 2004; Xu et al., 2006; Borlak et al., 2006). This difference in function could be reflected by the primary structure of these enzymes and an inspection of the amino acid sequences of all the human UGTs has indeed revealed an interesting observation. Specifically, the His residue near the N-terminus of the mature UGTs, His39 (UGT1A1 numbering, Fig. 8) is highly but not totally conserved in the human UGTs (as well as many related proteins), and it was recently shown to be involved in the catalytic activity of UGT2B7 (Miley et al., 2007). The only two sequences in which this His is replaced by another residue are UGT1A4 and UGT2B10 (Fig. 8). On the other hand, the replacements are quite different, a Pro in the case of UGT1A4, while in UGT2B10 it is a Leu, suggesting that the full explanation for the N-glucuronidation preference is likely more complex. In any case, since these deviations from

MOL # 37093

the conserved His residue occur within a conserved albeit short stretch of protein (Fig. 8), they may be significant for the preference of these UGTs for N-glucuronidation of suitable aglycones.

In conclusion, this work describes a set of observations and findings that solve the lingering question as to which one of the human UGTs is mainly responsible for the N-glucuronidation of nicotine, revealing for the first time that UGT2B10 is an important hepatic UGT with several xenobiotic substrates (nicotine and cotinine) rather than being an “orphan” enzyme. This work also demonstrates that the UGT2B subfamily of the human UGTs contains a member that specializes in N-glucuronidation reactions. These results open new research avenues, both towards a better understanding and possible manipulation of nicotine metabolism, as well as a deeper understanding of structure-function relationships among the UGTs.

### **Acknowledgements**

We would like to thank Johanna Mosorin, Marja Härmä, and Qin Hao for skillful technical assistance.

MOL # 37093

## References

- Borlak J, Gasparic A, Locher M, Schupke H, and Hermann R (2006) N-Glucuronidation of the antiepileptic drug retigabine: results from studies with human volunteers, heterologously expressed human UGTs, human liver, kidney, and liver microsomal membranes of Crigler-Najjar type II. *Metabolism* **55**:711-721.
- Finel M, Li X, Gardner-Stephen D, Bratton S, Mackenzie PI, and Radominska-Pandya A (2005) Human UDP-glucuronosyltransferase 1A5: identification, expression, and activity. *J Pharmacol Exp Ther* **315**:1143-1149.
- Ghosheh O, Vashishtha SC, and Hawes EM (2001) Formation of the quaternary ammonium-linked glucuronide of nicotine in human liver microsomes: identification and stereoselectivity in the kinetics. *Drug Metab Dispos* **29**:1525-1528.
- Ghosheh O and Hawes EM (2002a) N-glucuronidation of nicotine and cotinine in human: formation of cotinine glucuronide in liver microsomes and lack of catalysis by 10 examined UDP-glucuronosyltransferases. *Drug Metab Dispos* **30**:991-996.
- Ghosheh O and Hawes EM (2002b) Microsomal N-glucuronidation of nicotine and cotinine: human hepatic interindividual, human intertissue, and interspecies hepatic variation. *Drug Metab Dispos* **30**:1478-1483.
- Girard H, Thibaudeau J, Court MH, Fortier LC, Villeneuve L, Caron P, Hao Q, von Moltke LL, Greenblatt DJ and Guillemette C (2005) UGT1A1 polymorphisms are important determinants of dietary carcinogen detoxification in the liver. *Hepatology* **42**:448-457.
- Green MD and Tephly TR (1998) Glucuronidation of amine substrates by purified and expressed UDP-glucuronosyltransferase proteins. *Drug Metab Dispos* **26**:860-867.
- Hawes EM (1998) N+-Glucuronidation, a common pathway in human metabolism of drugs with a tertiary amine group. *Drug Metab Dispos* **26**:830-837.

MOL # 37093

Hukkanen J, Jacob P 3<sup>rd</sup>, and Benowitz NL (2005) Metabolism and disposition kinetics of nicotine. *Pharmacol Rev* **57**:79-115.

Kuehl GE and Murphy SE (2003) N-glucuronidation of nicotine and cotinine by human liver microsomes and heterologously expressed UDP-glucuronosyltransferases. *Drug Metab Dispos* **31**:1361-1368.

Kurkela M, Garcia-Horsman JA, Luukkanen L, Morsky S, Taskinen J, Baumann M, Kostianen R, Hirvonen J, and Finel M (2003) Expression and characterization of recombinant human UDP-glucuronosyltransferases (UGTs). UGT1A9 is more resistant to detergent inhibition than other UGTs and was purified as an active dimeric enzyme. *J Biol Chem* **278**:3536-3544.

Kurkela M, Patana AS, Mackenzie PI, Court MH, Tate CG, Hirvonen J, Goldman A, and Finel M (2007) Interactions with other human UDP-glucuronosyltransferases attenuate the consequences of the Y485D mutation on the activity and substrate affinity of UGT1A6. *Pharmacogenet Genomics* **17**:115-126.

Lévesque E, Turgeon D, Carrier JS, Montminy V, Beaulieu M, and Belanger A (2001) Isolation and characterization of the UGT2B28 cDNA encoding a novel human steroid conjugating UDP-glucuronosyltransferase. *Biochemistry* **40**:3869-3881.

Mackenzie PI, Gregory PA, Gardner-Stephen DA, Lewinsky RH, Jorgensen BR, Nishiyama T, Xie W, and Radomska-Pandya A (2003) Regulation of UDP glucuronosyltransferase genes. *Curr Drug Metab* **4**:249-257.

Mackenzie PI, Walter Bock K, Burchell B, Guillemette C, Ikushiro S, Iyanagi T, Miners JO, Owens IS, and Nebert DW (2005) Nomenclature update for the mammalian UDP glycosyltransferase (UGT) gene superfamily. *Pharmacogenet Genomics* **15**:677-685.

MOL # 37093

- Miley MJ, Zielinska AK, Keenan JE, Bratton SM, Radomska-Pandya A, Redinbo MR (2007) Crystal Structure of the Cofactor-Binding Domain of the Human Phase II Drug-Metabolism Enzyme UDP-Glucuronosyltransferase 2B7. *J Mol Biol* **369**:498-511.
- Nakajima M, Tanaka E, Kwon JT, and Yokoi T (2002) Characterization of nicotine and cotinine N-glucuronidations in human liver microsomes. *Drug Metab Dispos* **30**:1484-1490.
- Nakajima M and Yokoi T (2005) Interindividual variability in nicotine metabolism: C-oxidation and glucuronidation. *Drug Metab Pharmacokinet* **20**:227-235.
- Nishimura M, Naito S (2006) Tissue-specific mRNA expression profiles of human phase I metabolizing enzymes except for cytochrome P450 and phase II metabolizing enzymes. *Drug Metab Pharmacokinet* **21**:357-374.
- Radomska-Pandya A, Czernik PJ, Little JM, Battaglia E, and Mackenzie PI (1999) Structural and functional studies of UDP-glucuronosyltransferases. *Drug Metab Rev* **31**:817-899.
- Strassburg CP, Kneip S, Topp J, Obermayer-Straub P, Barut A, Tukey RH, Manns MP (2000) Polymorphic gene regulation and interindividual variation of UDP-glucuronosyltransferase activity in human small intestine. *J Biol Chem* **275**:36164-36171.
- Tukey RH and Strassburg CP (2000) Human UDP-glucuronosyltransferases: metabolism, expression, and disease. *Annu Rev Pharmacol Toxicol* **40**:581-616.
- Turgeon D, Chouinard S, Belanger P, Picard S, Labbe JF, Borgeat P, and Belanger A (2003) Glucuronidation of arachidonic and linoleic acid metabolites by human UDP-glucuronosyltransferases. *J Lipid Res* **44**:1182-1191.
- Uchaipichat V, Mackenzie PI, Guo XH, Gardner-Stephen D, Galetin A, Houston JB, Miners JO (2004) Human udp-glucuronosyltransferases: isoform selectivity and kinetics of 4-

MOL # 37093

methylumbelliferone and 1-naphthol glucuronidation, effects of organic solvents, and inhibition by diclofenac and probenecid. *Drug Metab Dispos* **32**:413-423.

Wells PG, Mackenzie PI, Chowdhury JR, Guillemette C, Gregory PA, Ishii Y, Hansen AJ, Kessler FK, Kim PM, Chowdhury NR, and Ritter JK (2004) Glucuronidation and the UDP-glucuronosyltransferases in health and disease. *Drug Metab Dispos* **32**:281-290.

Xu L, Krenitsky DM, Seacat AM, Butenhoff JL, Tephly TR, and Anders MW (2006) N-glucuronidation of perfluorooctanesulfonamide by human, rat, dog, and monkey liver microsomes and by expressed rat and human UDP-glucuronosyltransferases. *Drug Metab Dispos* **34**:1406-1410.

Zenser TV, Lakshmi VM, Hsu FF, and Davis BB (2002) Metabolism of N-acetylbenzidine and initiation of bladder cancer. *Mutat Res* **506-507**:29-40.

Zhang D, Zhao W, Roongta VA, Mitroka JG, Klunk LJ, and Zhu M (2004) Amide N-glucuronidation of MaxiPost catalyzed by UDP-glucuronosyltransferase 2B7 in humans. *Drug Metab Dispos* **32**:545-551.

MOL # 37093

## Figure legends

Fig 1. Chemical structures of nicotine, cotinine and their respective N-glucuronides.

Fig. 2. Detection of nicotine and cotinine glucuronidation by LC-MS. The chromatograms demonstrate the detection of glucuronides produced by incubations of 1mg protein/ml of recombinant UGT1A4 (microsomal membrane) or UGT2B10 (cell homogenate) in the presence of 0.5 mM of either nicotine (A) or cotinine (B) by the analytical methods described in this work (see Materials and Methods for details).

Fig. 3. Influence of microsomal membrane preparation on the normalized activity of recombinant UGT2B10. The glucuronidation rate of nicotine, 0.5 mM, by recombinant UGTs 1A4 and 2B10 was assayed using either microsomal membranes from the insect SF9 cells that were used to produce these enzymes, or in cell homogenates. The activities were determined in duplicates (< 10% difference) and the results were normalized according to the relative amount of immuno-detectable UGT in each sample (see Materials and Methods for further details).

Fig 4. Glucuronidation activity of recombinant human UGTs 1A4, 1A9, 2B7 and 2B10 towards nicotine (A) and cotinine (B). Three different substrate concentrations were used in each case and the activity rates were normalized to the relative expression level of each recombinant UGT (see Methods for further details). Activities were determined in duplicate (<10% difference). N.D., no detectable activity or activity below quantification limit (0.04 pmol/min/mg for nicotine and 0.08 pmol/min/mg for cotinine).

MOL # 37093

Fig 5. Kinetic analyses of the glucuronidation of nicotine (A) and cotinine (B) by human liver microsomes (HLM) and recombinant human UGT1A4 and UGT2B10. The glucuronidation rates,  $v$ , for the HLM are presented on the left hand side Y axis, while the right hand side values are for the non-normalized rates of the recombinant UGT samples. The rates represent the mean ( $\pm$ S.D.) of 2-4 independent determinations. The calculated  $K_m$  ( $\pm$ S.E.) values for the substrate, derived from the Michaelis-Menten equation, are also presented (See Methods for further technical details).

Fig 6. mRNA expression levels of the identified nicotine glucuronidating enzymes in human tissues. Total RNA was extracted from human liver (47 donors pooled), kidney, stomach, small intestine (5 donors pooled), colon (3 donors pooled), trachea, lung, and whole brain. Quantitative reverse transcription PCR was then performed using primers specific for UGT2B10, UGT1A4, UGT2B7, and 18S rRNA (for normalization), and quantified by use of standard curves. Bars represents the mean (S.E.) of 3 independent reverse transcription reactions performed for each tissue. N.D., no detectable mRNA.

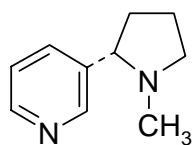
Fig 7. Activity analyses of human microsomes from either the liver (A) or intestine (B. the microsomes were from the duodenum and jejunum sections of the intestine) in N-glucuronidation of nicotine and cotinine. Three different substrate concentrations were used in the assays. Note the differences in Y axis units between panels A and B. Activities were determined in duplicate (<10% differences). N.D., no detectable activity or activity below quantification limit (0.04 pmol/min/mg for nicotine and 0.08 pmol/min/mg for cotinine).



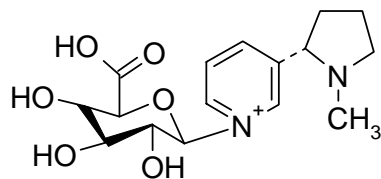
MOL # 37093

Fig 8. Sequence alignment of N-terminal 51-60 amino acids of all the human UGTs. The highly but not strictly conserved His residue, H39 in the case of UGT1A1, is indicated by bold face and italic style fonts. The starting point of the mature UGTs sequence and the signal sequences the precedes it are also indicated. The stars at the bottom indicate residues that are fully conserved among the human UGTs (see Mackenzie et al., 2005) for the source of the sequences, including UGT2A2).

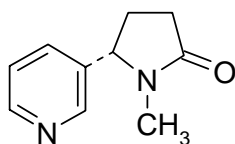
Fig. 1.



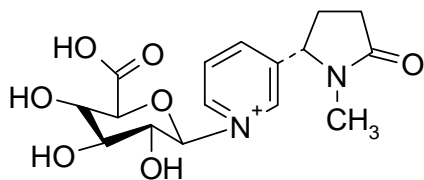
Nicotine



Nicotine *N*-glucuronide



Cotinine



Cotinine *N*-glucuronide

Fig. 2.

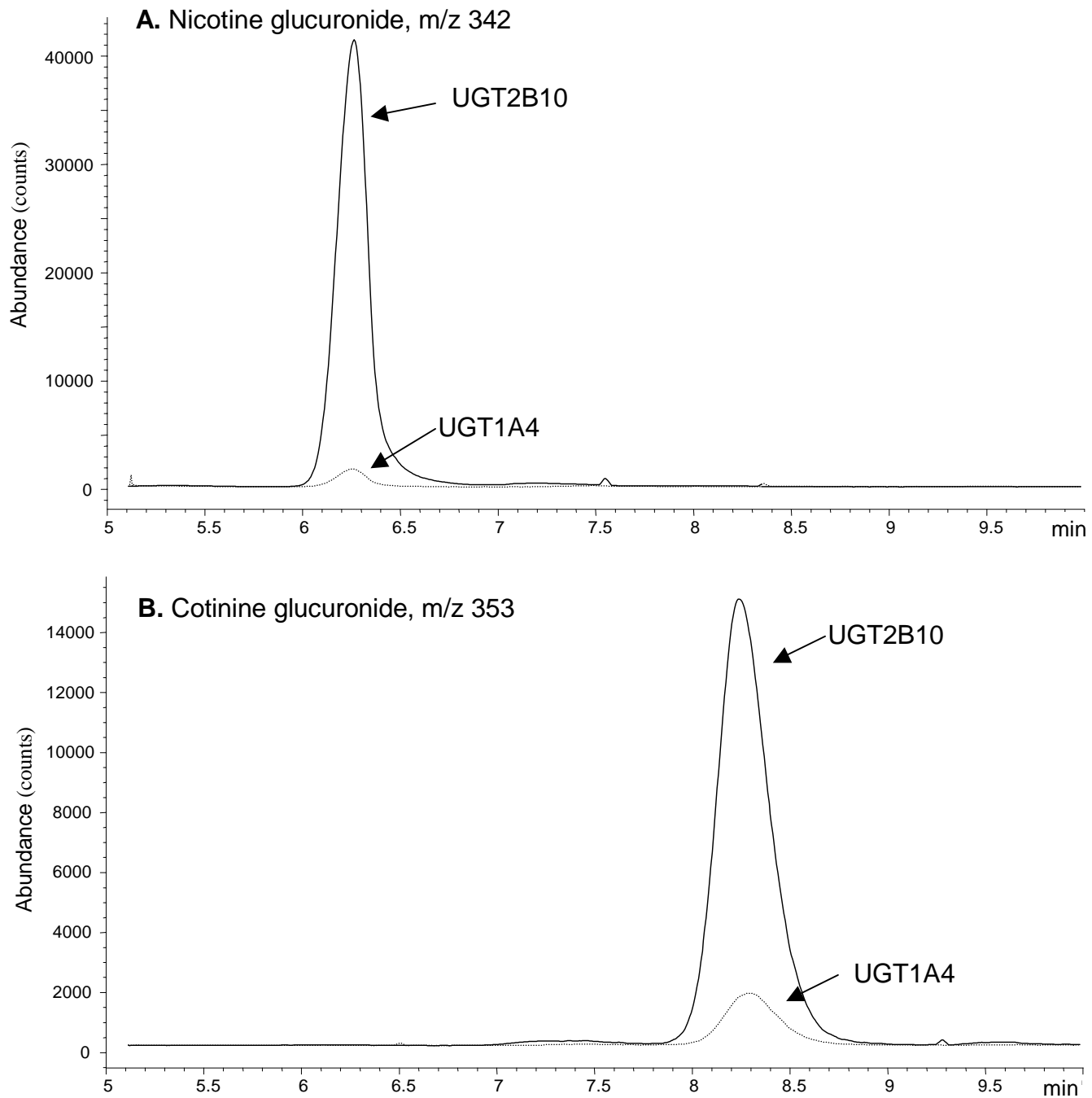


Fig. 3.

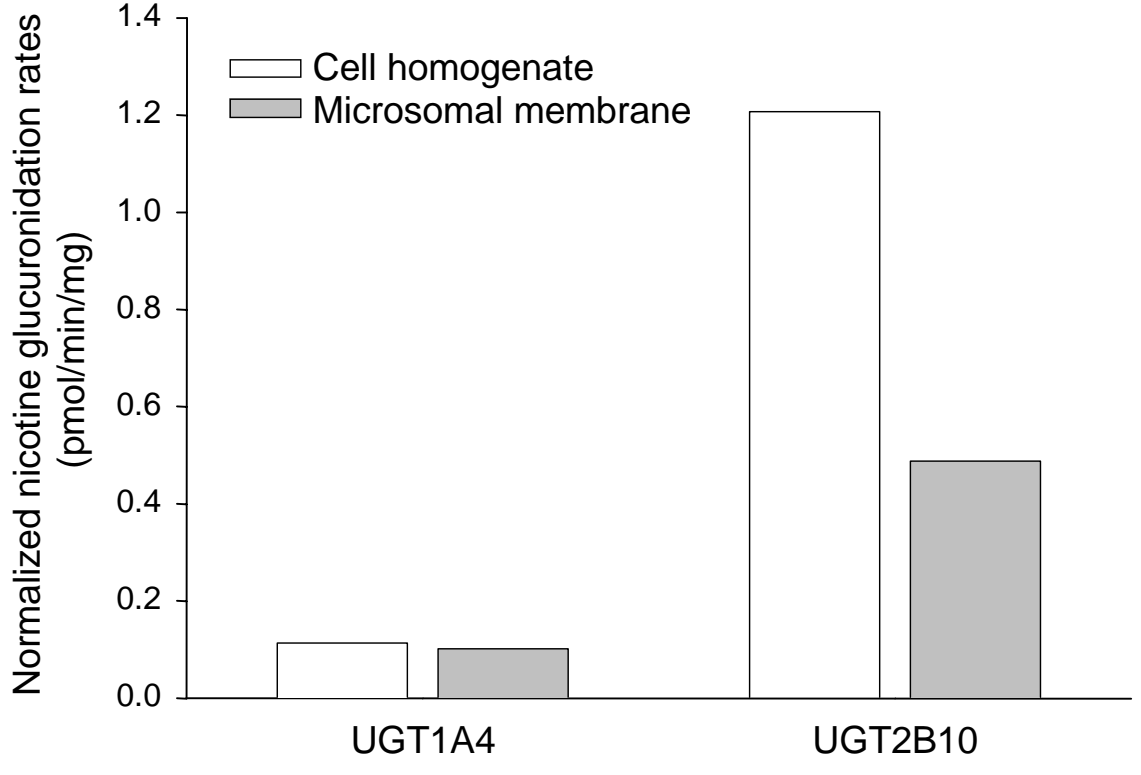


Fig. 4A.

### A. Nicotine

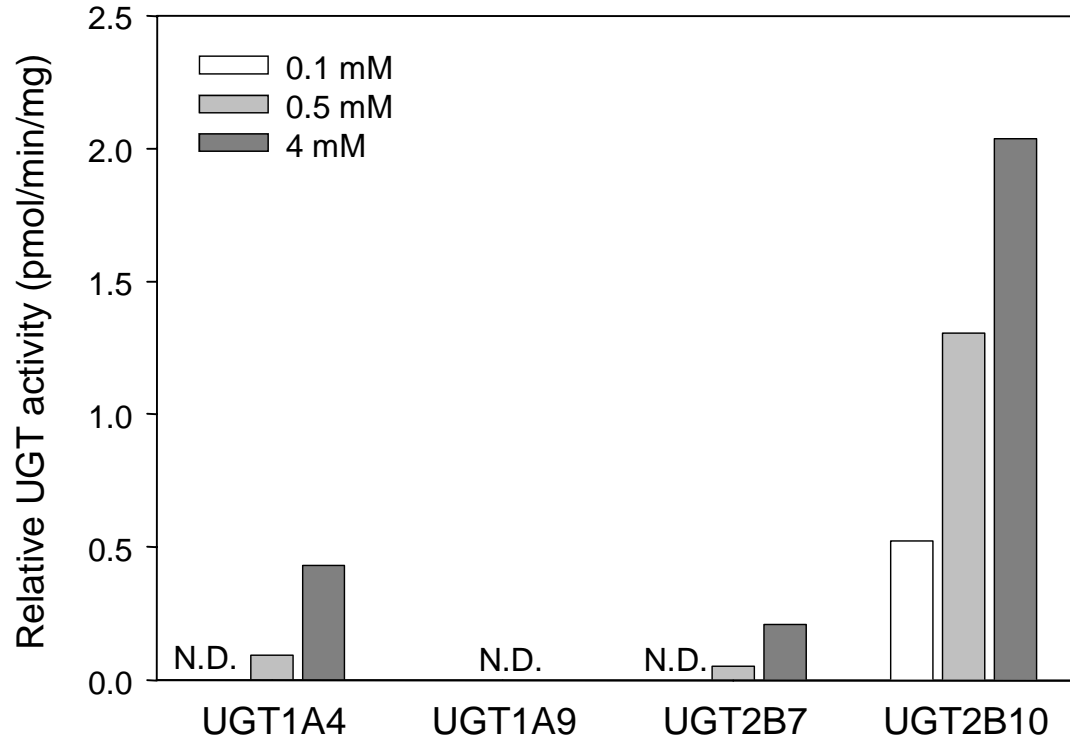


Fig. 4B.

### B. Cotinine

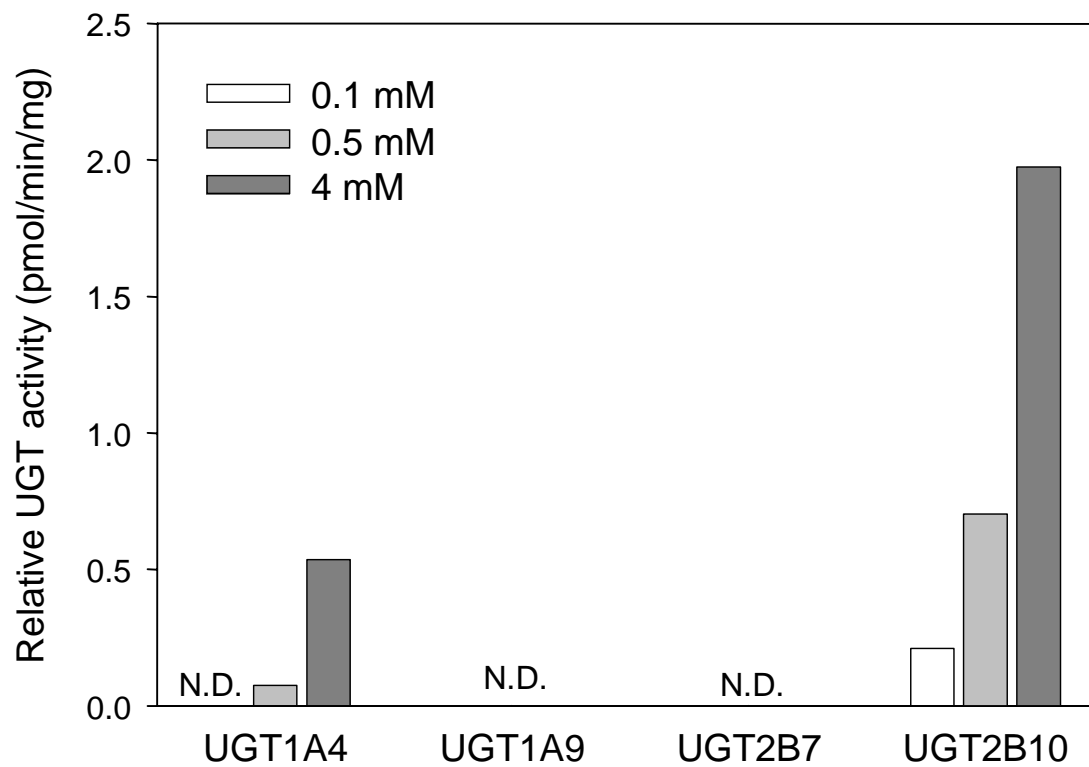


Fig. 5A.

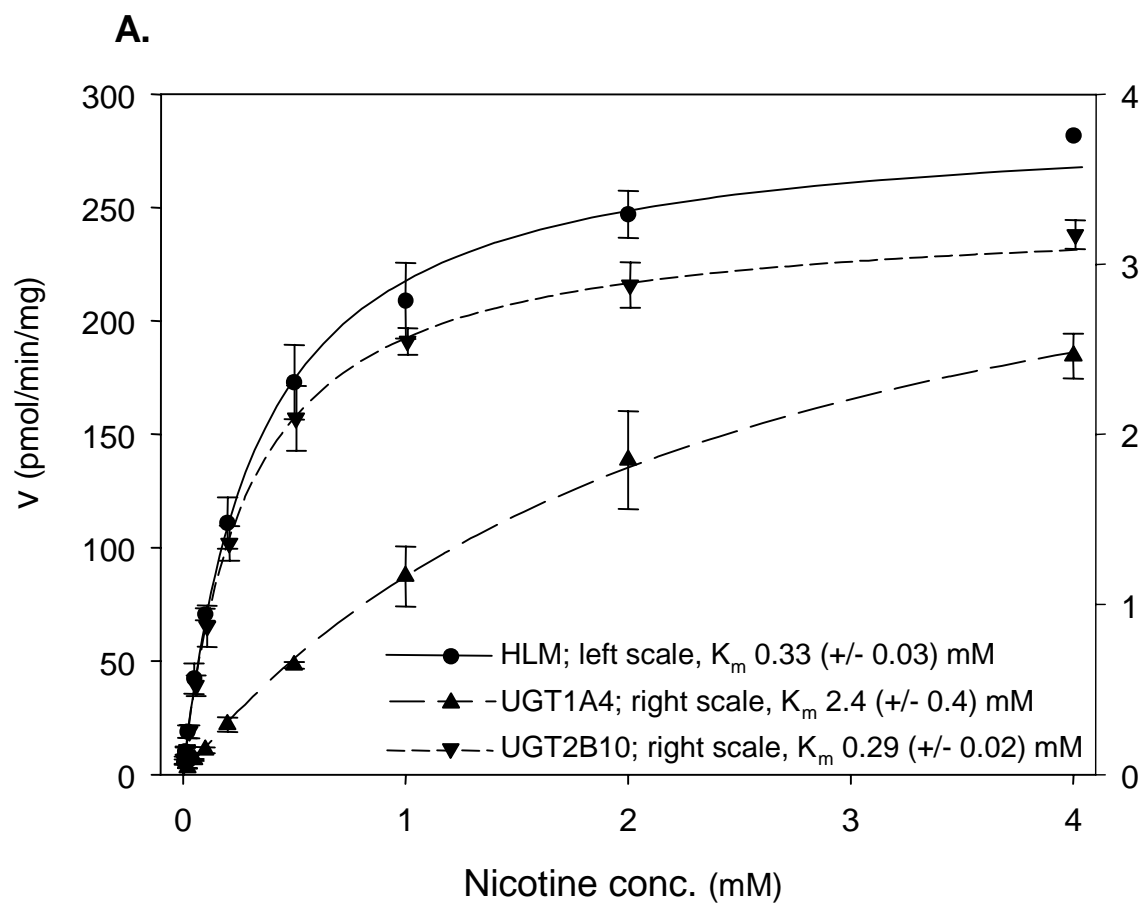


Fig. 5B.

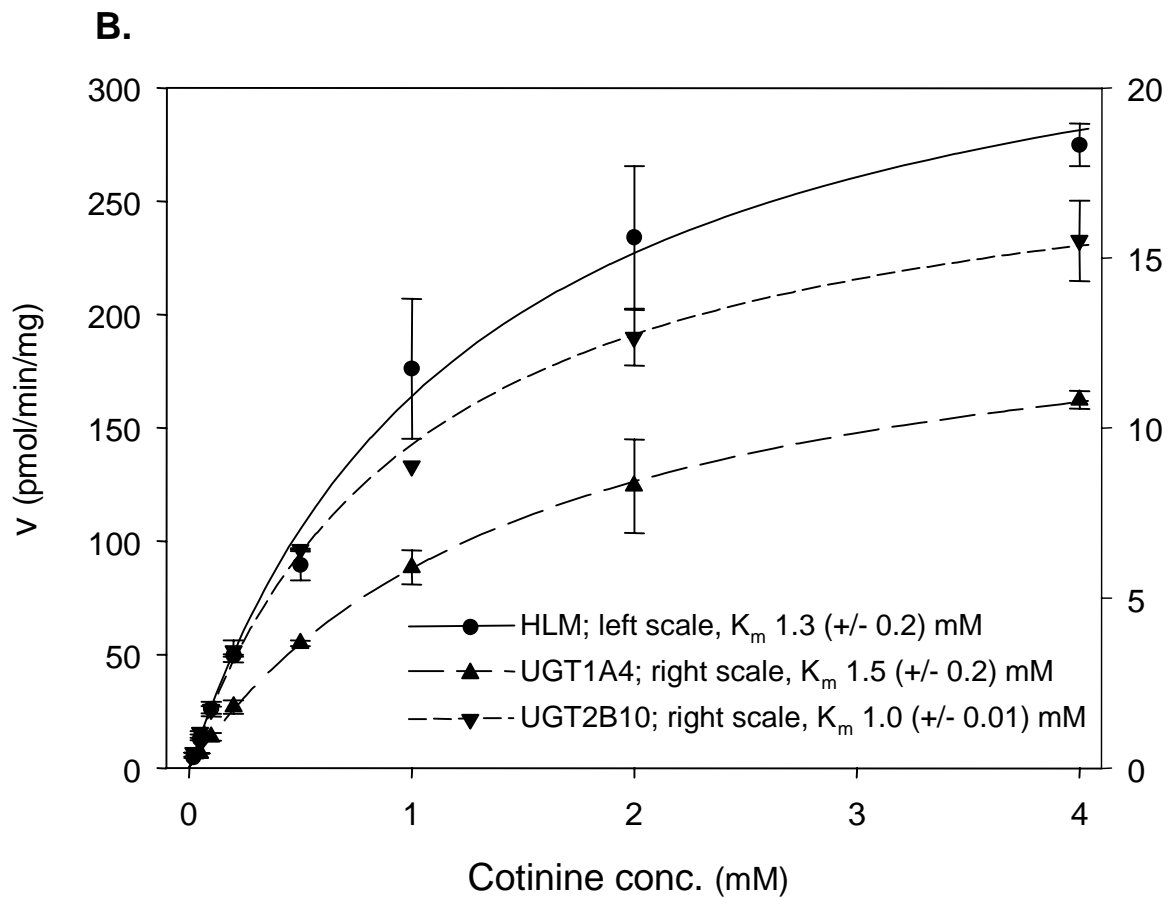




Fig. 6.

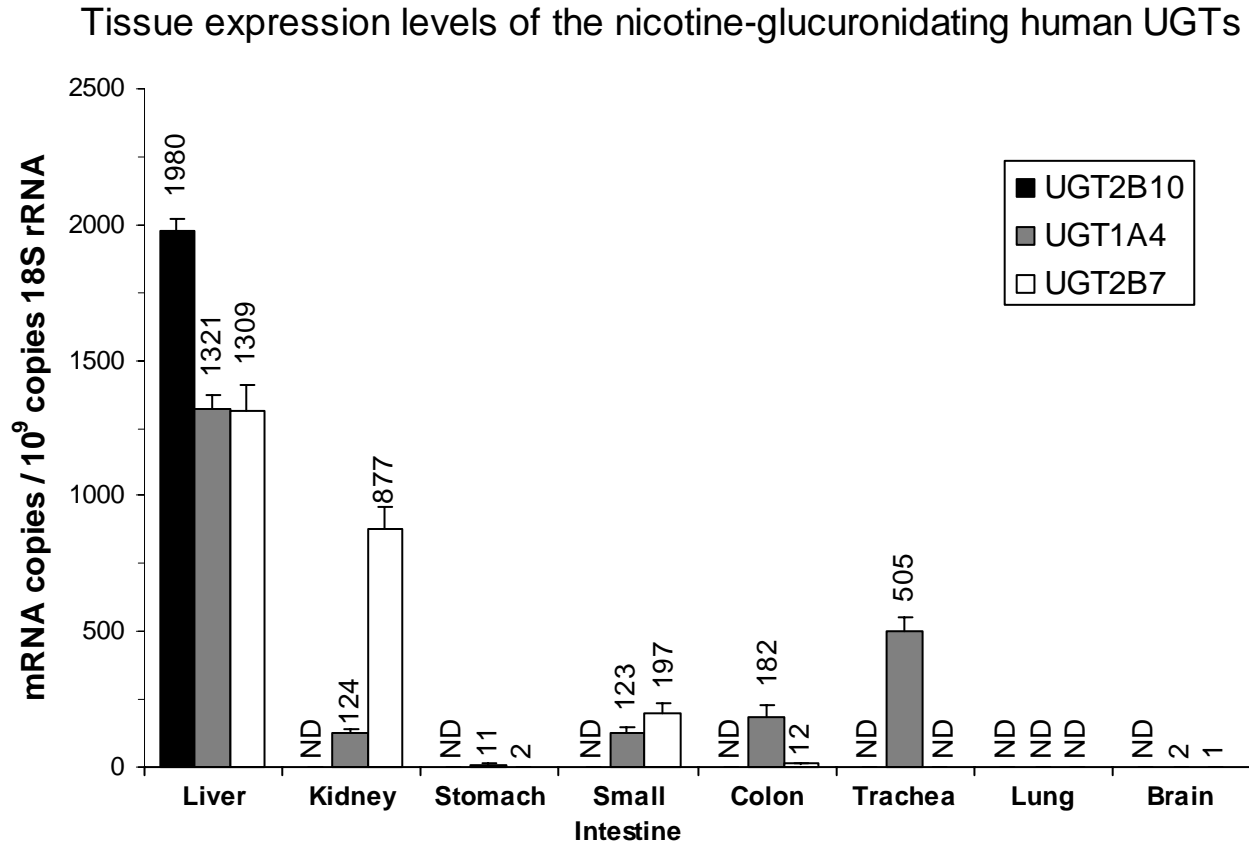


Fig. 7.

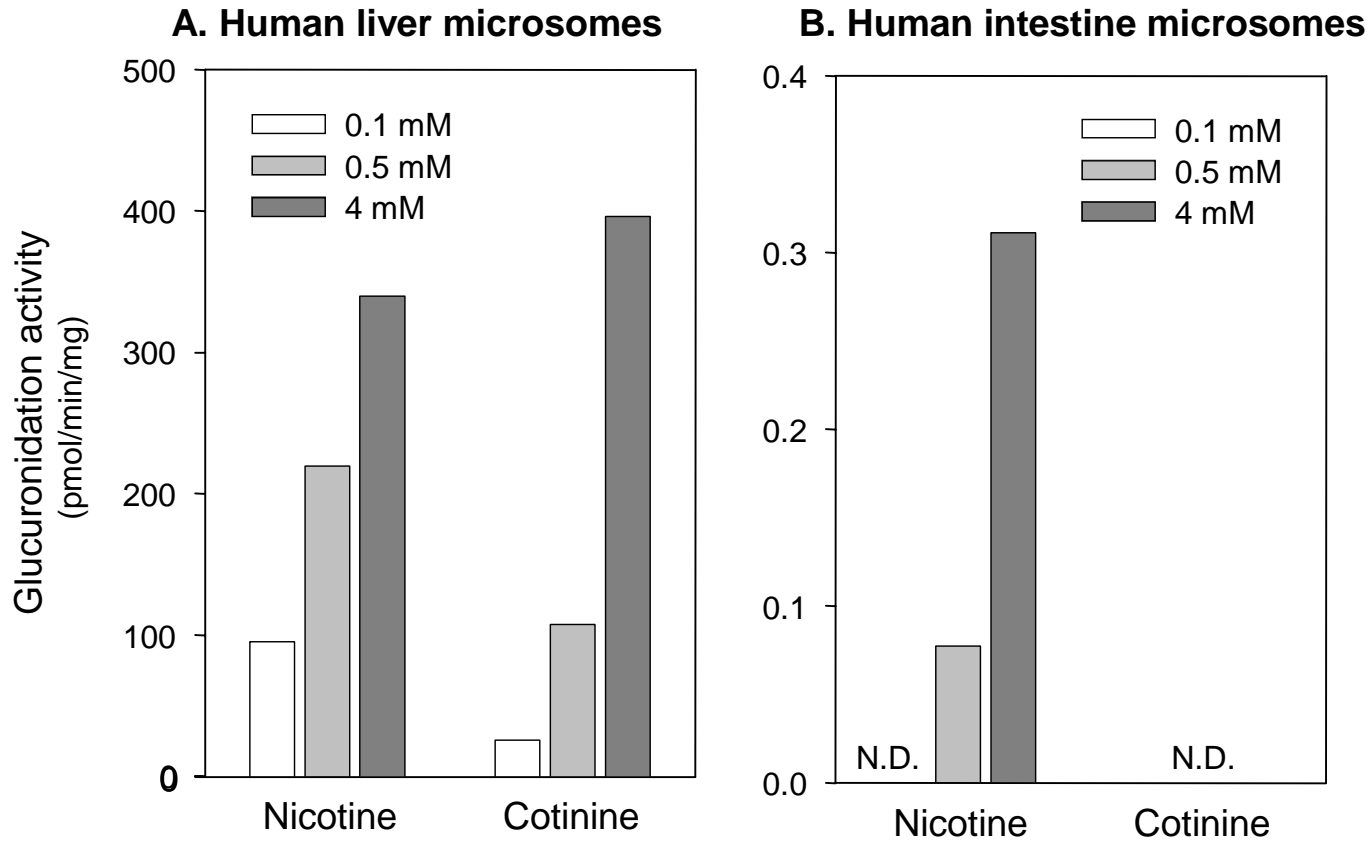


Fig. 8.

	Signal sequences	Mature proteins	H39 (1A1 numbering)																		
1A1	MAVESQGG	RPLVLG	LLLCV	LGPV	VSHAGK	ILLIP	VDGS	<b>HW</b> LSMLGAIQQ	LQ	RGHEIV	58										
1A3	MATGLQV	PLPWL	ATGL	LLLL	SVQP	WAESG	KVLV	VPID	GS	<b>HW</b> LSMREVL	RELH	ARGH	QAV	59							
<b>1A4</b>	MARGLQV	PLPRL	ATGL	LLLL	SVQP	WAESG	KVLV	VP	TDGS	PWLSM	REAL	RELH	ARGH	QAV	59						
1A5	MATGLQV	PLPQL	ATGL	LLLL	SVQP	WAESG	KVLV	VP	TDGS	<b>HW</b> LSM	REAL	RDLH	ARGH	QVV	59						
1A6	MACLLRS	FQRIS	AGV	FFL	ALW	GMMV	VDK	LLV	VP	QDGS	<b>HW</b> LSM	KDIVE	VLS	DRGHEIV	57						
1A7	MARAGWT	GLLPL	VCL	LLT	TCG	FAK	AGK	LLV	VP	MDGS	<b>HW</b> FTMQ	S	VVEK	LILRGHEVV	56						
1A8	MARTGWT	SPIPL	CVS	LLT	TCG	FAE	AGK	LLV	VP	MDGS	<b>HW</b> FTMQ	S	VVEK	LILRGHEVV	56						
1A9	MACTGWT	SPLPL	CVS	LLT	TCG	FAE	AGK	LLV	VP	MDGS	<b>HW</b> FTMR	S	VVEK	LILRGHEVV	56						
1A10	MARAGWT	SPVPL	CVS	LLT	TCG	FAE	AGK	LLV	VP	MDGS	<b>HW</b> FTMQ	S	VVEK	LILRGHEVV	56						
2B4	MSMKWTS	SALLL	IQL	SCY	FSS	GSC	GKVL	VWP	TEFS	<b>HW</b> MNI	K	TIL	DEL	VQRGHEVT	54						
2B7	MSVKWTS	VILLI	IQL	SFC	FSS	GNC	GKVL	VW	AAEYS	<b>HW</b> MNI	K	TIL	DEL	IQRGHEVT	54						
<b>2B10</b>	MALKWTT	VLLI	IQL	SFY	FSS	GSC	GKVL	VW	AAEYSL	<b>HW</b> MNM	K	TIL	KEL	VQRGHEVT	53						
2B11	MTLKWTS	VLLLI	IHL	SCY	FSS	GSC	GKVL	VW	AAEYS	<b>HW</b> MNM	K	TIL	KEL	VQRGHEVT	54						
2B15	MSLKWTS	VFLLI	IQL	SCY	FSS	GSC	GKVL	VWP	TEYS	<b>HW</b> INM	K	TILE	EEL	VQRGHEVT	54						
2B17	MSLKWMS	VFLLM	QLS	CYF	S	GSC	GKVL	VWP	TEYS	<b>HW</b> INM	K	TILE	EEL	VQRGHEVI	54						
2B28	MALKWTS	VLLLI	IHL	GCY	FSS	GSC	GKVL	VW	TGEYS	<b>HW</b> MNM	K	TIL	KEL	VQRGHEVT	54						
2A1	MLNNLLL	FSLQ	ISL	IGT	T	LGG	NVLI	W	PMEGS	<b>HW</b> LNV	KI	I	DEL	IKKEHNV	51						
2A2	MVSIRD	F	TMP	KKF	VQ	MLV	FNLT	L	TEV	VLS	GNV	LIW	P	DGS	<b>HW</b> LNI	KI	I	LEEL	IQRN	HNV	60
2A3	MRSDK	SALV	FLL	QLF	CV	G	CGF	CGK	VLV	WP	CDMS	<b>HW</b> LNV	KV	I	LEEL	I	VRG	HEVT	54		
										*		*	*		*		*				